Received: 23 May 2020 | Revised: 11 January 2021 | Accepted: 12 January 2021
DOI: 10.1002/pip.3396

APPLICATION

WILEY PROGRESS IN PHOTOVOLTAICS

Temperature coefficients of degraded crystalline silicon photovoltaic modules at outdoor conditions

M. Piliougine[1] | A. Oukaja[2] | M. Sidrach-de-Cardona[3] | G. Spagnuolo[1]

[1]Dipartimento di Ingegneria dell'Informazione ed Elettrica e Matematica Applicata/DIEM, University of Salerno, Via Giovanni Paolo II 132. 84084 Fisciano (SA), Italy

[2]Master student, Universidad Internacional de Andalucía, 29007 Málaga, Spain

[3]Departamento de Física Aplicada II, Universidad de Málaga, 29071 Málaga, Spain

Correspondence
M. Piliougine, Dipartimento di Ingegneria dell'Informazione ed Elettrica e Matematica Applicata/DIEM, University of Salerno. Via Giovanni Paolo II 132. 84084 Fisciano (SA), Italy.
Email: mpiliouginerocha@unisa.it

Funding information
Ministerio de Ciencia, Innovación y Universidades, Spain, Grant/Award Number: RTI2018-095097-B-I00

Abstract

The temperature effect on photovoltaic modules is usually quantified by means of some coefficients relating the variations of the open-circuit voltage, of the short-circuit current, and of the maximum power to temperature changes. In this paper, comprehensive experimental guidelines to estimate the temperature coefficients when measurements are performed outdoors are given. In addition, a correction procedure is applied to the short-circuit current to cancel out the influence of the fluctuations in the irradiance level. The experimental results shown in this paper refer to several single-crystalline silicon modules that have been operating for 21 years. Consequently, the estimated values of the temperature coefficients also account for module ageing processes. The coefficients of determination achieved in the case of the temperature coefficients of the open-circuit voltage and the maximum power are very close to one. Results concerning the temperature coefficients of the short-circuit current are also suitable if they are previously corrected.

KEYWORDS
electrical parameter, outdoor measurements, photovoltaic degradation, temperature coefficient

1 | INTRODUCTION

The performance of a photovoltaic (PV) module depends on the environmental conditions, mainly on the global incident irradiance G on the module plane. However, the temperature T of the p–n junction also influences the main electrical parameters: the short-circuit current I_{SC}, the open-circuit voltage V_{OC}, and the maximum power P_{max}. The first studies about the behavior of PV cells under varying conditions of G and T date back several decades ago.[1-4] In general, it is known that V_{OC} shows a significant inverse correlation with T, whereas for I_{SC} that correlation is direct, but weaker, so that this increment does not compensate for the decrease of V_{OC}. As a consequence, P_{max} reduces when T increases. This correlation between the output power of a solar cell and its junction working temperature depends on the semiconductor material,[2] and it is due to the influence of T on the concentration, lifetime, and mobility of the intrinsic carriers, that is, electrons and holes, inside the PV cell.

The temperature sensitivity is usually described by some temperature coefficients, each one expressing the derivative of the parameter it refers to with respect to the junction temperature. The values of these parameters can be found in any PV module data sheet; they are the following:

- β Coefficient of variation of V_{OC} with respect to T, given by $\partial V_{OC}/\partial T$.
- α Coefficient of variation of I_{SC} with respect to T, given by $\partial I_{SC}/\partial T$.
- δ Coefficient of variation of P_{max} with respect to T, given by $\partial P_{max}/\partial T$.

Some manufacturers provide β_{rel}, α_{rel}, and δ_{rel}, in 1/°C or in %/°C, by expressing their values in relative terms through a normalization by $V_{OC}|_{25°C}$, $I_{SC}|_{25°C}$, and $P_{max}|_{25°C}$, respectively. Although these coefficients could depend on T, according to,[4] in the typical range of the operating temperatures for terrestrial applications, the effect of T can be neglected, because α and β values are almost invariant with the temperature.

A reliable estimation of the temperature coefficients requires an accurate measurement of the p–n junction temperature, which is a quite involved task.[5] Indeed, for commercial PV modules: (1) it

is not possible to attach a sensor in direct contact with the cells, and (2) each cell works at its own temperature, so there is not a unique junction temperature for the whole module. As it is shown in previous literature,[6-10] the followed approach to estimate these temperature coefficients is through the plot of the electrical parameter of interest versus the module temperature, and then performing a linear regression, being the slope of the line the corresponding temperature coefficient. This method works well enough with β and δ, but the results with α are unsatisfactory, because the module temperature is a second-order factor, being the irradiance the main influential one: Any fluctuation of the irradiance will have a strong influence on the current, overlapping the effect of the temperature. Therefore, in order to estimate α, it is mandatory to keep the irradiance level during the measurement as constant as possible. This requirement is not hard to satisfy if a solar simulator is used, but it is hard to get it under outdoor conditions. Sometimes, the values for α obtained indoors can differ from the ones obtained outdoors.[11,12] This is due to the temperature dependency of the spectral response of c-Si,[13] implying a change of spectral mismatch. However, these coefficients can be measured using simulated light following the work by Salis et al.[14]

This paper is mainly aimed at presenting some guidelines for estimating the temperature coefficients of commercial PV modules through experimental measurements. The latter ones are performed in the real PV modules operating conditions, thus outdoors and not in laboratory through solar irradiance simulators and climatic chambers. Therefore, this paper will be very useful for anyone that needs to estimate the temperature coefficients without having indoor facilities, which are very expensive. In the paper, a wide discussion about the way of minimizing all the sources of uncertainty due to the outdoor measurements is given. This analysis allows to have results with the maximum coefficient of determination in the regression procedure. In addition to a series of practical recommendations when performing the experiments, a correction procedure is applied to the measured values of I_{SC} to improve its correlation with T. The modules used in the experiments have been operating in a real PV plant for more than two decades. This has allowed an analysis of the correlation between possible degradation effects and the values of the temperature coefficients.

The paper is organized as follows. In Section 2 an overview of the literature concerning the measurement of the temperature coefficients and their dependency on the operating conditions of the PV module is given. The nameplate data and a brief description of the measurement system can be seen in Section 3. The methodology employed to estimate the different temperature coefficients is provided in Section 4, including an analysis of the uncertainties. In Section 5 the main results are summarized and the main achievements are discussed. Finally, the main conclusions of this work can be found in Section 6.

2 | STATE OF THE ART

The most widely used curve translation procedure, described by IEC,[10] was actually published many years ago by Sandstrom.[15] In this early publication, the proposed method adopts some of the temperature coefficients defined in Section 1 but no practical methodology to estimate them is suggested therein.

Fortunately, the original[10] includes two procedures aimed at estimating the temperature coefficients α, β, and δ: one specifically to be used with natural sunlight, on which this article is based, and another that assumes that a solar simulator is available. Following this last approach described in the standard, many advantages can be achieved. With an artificial lamp, the target irradiance level can be set straightforwardly. In addition,the IEC[10,16] requires some type of control mechanism to change the temperature of the PV module. In this way, it is possible not only to fix exactly the desired temperature but also to achieve a high degree of temperature uniformity (not possible outdoors) minimizing the uncertainties. Moreover, the temperature increments can be programed to be equispaced (avoiding biasing the regression line) and we can span the range to a very wide interval of temperatures regardless the weather, season and location.

Additional information related to the specific specifications of the solar simulator to be used is defined by the IEC.[17] There are different types of simulator, and the measurement system is usually integrated. Even in some models, different flashes are applied to measure individual points of the I–V curve. Some of the critical features are the spectral match to AM1.5 defined by the IEC,[18] the non-uniformity of the irradiance over the PV module, and the instability of level of the irradiance. Despite these problems, the estimation of the temperature coefficients indoors is by far much easier and less uncertainty is associated to the results.

Arora and Hauser[19] mathematically calculate the temperature coefficients for a typical crystalline silicon cell. In principle, the behavior of the electrical performance is not linear with temperature, as it was also confirmed later by Fan.[20] This work reports different values for α and δ depending whether a spectral distribution AM0 (before passing the atmosphere) or AM1 (at Earth surface with normal incidence) is considered, whereas the same results are obtained in both cases for β.

Osterwald et al.[6] perform an experimental comparative analysis of the temperature coefficients of several types of PV cells. The measurement system, described by,[21] was based on a bipolar power supply and two high-resolution multimeters for acquiring the current–voltage pairs. The PV cells were tested in laboratory by using a calibrated solar lamp and a thermo-electric plate to control the temperature. Two different silicon-based cells are studied; they show similar β values but significant differences in terms of α and δ.

Landis[22] gives a survey about the temperature coefficients referred to many different PV cells technologies. All technologies show a linear positive correlation between T and I_{SC}, so that $\alpha > 0$, and a negative linear relationship between T and V_{OC}, thus $\beta < 0$. Instead, the maximum power, as well as the fill factor, might exhibit a non-linear trend when a wide range of temperature of several tens of degrees Kelvin is considered: This phenomenon becomes more evident for some technologies different from crystalline silicon. Results concerning the temperature coefficient α are quite heterogeneous: Those ones obtained by using extraterrestrial data, by a solar simulator, or under real operating conditions appear to be significantly different, because the spectral distribution of the irradiance is not the same from case to case.

When several crystalline silicon cells are compared by Emery and Osterwald,[7] there are significant discrepancies in the estimation of β and δ, whereas the α estimations are completely different, some being even five times the value of others. It is worth to note that the

measured value of α depends on the spectrum of the light hitting on the cells. This is demonstrated by Dupré and Vaillon[11] or Osterwald et al.[12]

The temperature sensitivity of the current I_{Pmax} and voltage V_{Pmax} in the maximum power point is analyzed by King et al.[8] A formula relating both coefficients to δ is given. Many aspects related to the experimental measurements are discussed: the non-uniformity of the temperature among the cells in a PV module, temperature measurement errors due to the effect of the wind, the undesired instability of the irradiance level during the measurements, and others.

Fanney et al.[9] present the results of experimental measurements performed on three PV modules of different technologies. They are installed outdoors and are tested using two different facilities, each one equipped with a solar tracker, a pyranometer, some temperature sensors, an anemometer, and its own *I*–*V*curve tracer. The results from both facilities show a high discrepancy, especially affecting α, which assumes small values.

Makrides[23] experimentally determine the temperature coefficients of several PV grid-connected plants using different PV technologies. A commercial capacitive *I*–*V* curve tracer is used to perform the measurements, whereas the temperature change is achieved by covering and by uncovering the PV modules. A further long-term approach, which is based on the data stored by the grid connected inverters, has been also proposed. A drawback of that approach is that it is only able to estimate the temperature coefficients of P_{max}, V_{Pmax}, and I_{Pmax}.

Smith et al.[24] determine α, β, and δ for twelve types of crystalline PV modules from five different manufacturers. A huge database of *I*–*V* curves over a long time period and with different outdoor conditions has been processed. The *I*–*V* curves obtained with *G* values falling within a narrow range are analyzed, and linear regressions are performed to estimate the temperature coefficients. That approach requires a long measurement time, because *I*–*V* curves at similar *G* values but at different *T* must be acquired. Moreover, the use of measurements obtained in different days adds a further source of uncertainty in the evaluation of α.

Several modules from three different technologies, installed on two-axis sun trackers at two different locations, are measured, and the temperature coefficients are calculated by Granata et al.[25] Different measurement systems have been used: a commercial capacitive curve tracer and an experimental system based on a set of laboratory instruments. The thermal insulation of the module back surface is proven to be useful to make the temperature of the modules more uniform and to expand the upper limit of the temperature range. The experimental results reveal a high variability of the α values and a more repeatable set of values for β.

Very recently, Coftas et al.[26] propose a comparative analysis of the temperature coefficients for some of the PV technologies used nowadays. The influence of the irradiance level on the temperature coefficients is also estimated, and the results are compared to previous literature. The tests are performed under single cells or small modules using the custom laboratory equipment described in a previous paper,[27] which can use an artificial light source or natural sunlight. A comparison among the values determined for β by referring to the same type of cells reveals that there is a significant coherence. The same cannot be said for the other thermal coefficients.

It is worth noting that the *long-term* effect on the temperature coefficients due to degradation has not been widely investigated in literature. In previous literature,[28-30] the variation of the temperature coefficients due to the potential-induced degradation (PID) has been documented. As for the light-induced degradation (LID), Berthod et al.[31] show a variation of all the temperature coefficients.

3 | EXPERIMENTAL SETUP

The experimental activity has been carried out at the *Laboratory of PV Systems* of the *School of Telecommunication and Computer Engineering* of the *University of Málaga* (Spain). Nine PV modules Isofotón I–53[32] are the subject of the measurements shown in the following. The modules are part of a PV generator connected for 21 years at the input of a grid tied inverter. As a consequence, the following results refer to PV modules that are to some extent degraded. The sc-Si modules under study have a nominal STC (Standard Test Conditions: irradiance of 1,000 W/m^2, cell temperature of 25°C, and a spectral distribution AM1.5) peak power equal to 53 W and include 36 cells connected in series, which are physically distributed in 3 rows and 12 columns. The PV cells are laminated between several layers of encapsulating materials: first a layer of glass, then a layer of EVA (ethylene vinyl acetate), and then the cells thereof. After, there is another layer of EVA and a final layer of Tedlar®. The nameplate data of the PV modules provided by the manufacturer are shown in Table 1.

Although many manufacturers include the temperature coefficients β, α, and δ (or their respective normalized values) in the specification sheets, at the time when this module was in production, Isofotón did not provide any temperature coefficient. However, through an internal communication with the staff of the R&D Department of Isofotón a few years ago, it was possible to know the values of the temperature coefficients included in Table 1, measured over a new PV module of the same model by a laboratory of TÜV Rheinland. Unfortunately, that new module does not belong to the same production batch of the test

TABLE 1 Specifications of the photovoltaic modules

General features	
Manufacturer	Isofotón
Model	I–53
Technology	Single-crystalline silicon
Number of cells in series	36
Number of strings in parallel	1
Weight	5.5 kg
Total dimensions	1304 × 340 × 39.5 mm
Cell area	104.4 cm^2
NOCT	47 °C
Electrical parameters	
Maximum power P_{max}	53 W ± 10%
Short-circuit current I_{SC}	3.27 A
Open-circuit voltage V_{OC}	21.6 V
Current at MPP I_{Pmax}	3.05 A
Voltage at MPP V_{Pmax}	17.4 V
Temperature coefficients	
V_{OC} temperature coefficient (β_{STC})	−80 mV/°C
I_{SC} temperature coefficient (α_{STC})	+1.29 mA/°C
P_{max} temperature coefficient (δ_{STC})	−256 mW/°C

modules under study. TÜV Rheinland has estimated the temperature coefficients using a solar simulator over a temperature interval of 30°C scanned during 10 minutes. They report that these values provided in the last three rows of Table 1, in addition to the coefficients of determination R^2 for α, β ,and δ, were 0.7555, 0.9991 and 0.9992, respectively.

Each PV module that is the subject of the experimental measurements is mounted on a two-axis solar tracker to the aim of having an angle of incidence of the solar rays that is as much close to zero as possible. The meteorological variables are acquired by a weather station composed of an anemometer and a wind vane (Young 03002L), a combined sensor of air temperature and relative humidity (Young 41382LC) and two irradiance sensors on the module plane: a thermo-electric pyranometer EKO MS-80A (with a nominal time response of 2 s), and a calibrated reference PV cell identical to those ones used in the tested modules. This PV cell, which is an Isocell 103, has a short-circuit current $I_{SC,STC} = 3.126$ A at STC. The terminals of the cell have been short-circuited using a shunt of very low resistance and exact known value (150 mV for 4 A) with calibration certificate (from the voltage drop across the shunt resistor it is possible to calculate $I_{SC,ref}$).

In order to measure cell temperature, there are available four Pt100 Resistance Temperature Detectors (RTD) using a four-wire connection to avoid ohmic losses. These sensors are encapsulated by a silicone sheath allowing a better coupling to the back surface of the PV modules. Due to edge and corner effects, the actual temperature of the different cells of the module could be different. Therefore, the temperature to use in the regression procedure is determined calculating the average value from the measurements provided by these four temperature sensors (the IEC[10] provides a figure suggesting four specific positions of a PV module). The output signals of all these sensors are connected to a Compact FieldPoint™ cFP-2120 controller and acquisition system from National Instruments.

The *I*–*V* curve acquisition system was described in a previous paper[33]: a four-quadrant power supply performs the voltage sweep at the PV module terminals in a suitable voltage range. The *I*–*V*samples are acquired by a pair of multimeters triggered by a common square signal to ensure the simultaneity of both readings. The acquired *I*–*V* curves are stored in a relational database (MySQL) and can be downloaded and exported for further treatment through a web application.[34]

4 | METHODOLOGY

4.1 | Measurement procedure and recommendations

In order to provide a full vision of the proposed procedure, Figure 1 depicts a flow chart of the main steps to follow. In order to determine the temperature coefficients α, β, and δ, a series of*I*–*V* curves of each PV module have to be measured and processed. A number of consecutive *I*–*V* curves are acquired as fast as possible, while the module temperature increases from an initial value to a higher steady state one. It is very important to explore a module temperature range that is wide enough. Therefore, each module under test has been cooled down as much as possible by keeping it inside a dark and cooled

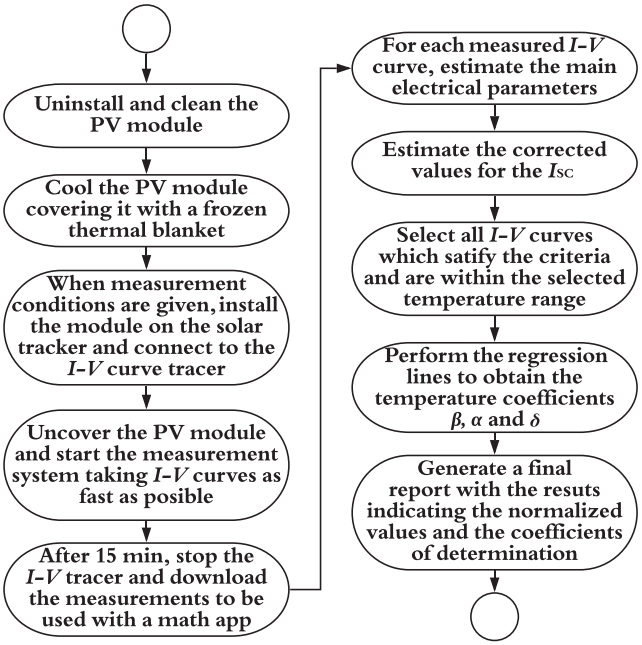

FIGURE 1 Flow chart describing the proposed procedure

room, wrapped into a thermal blanket that has been previously stored in a freezer. Once reached the desired thermal conditions, the PV module is installed on the solar tracker as fast as possible, the thermal blanket is removed and the batch of measurements is then started. The sun radiation increases the module temperature until thermal equilibrium is reached. By means of the approach just described, an initial module temperature even lower than 23°C can be achieved, and in a summer day in Málaga, a final steady state temperature close to 48°C is reached. The maximum temperature reached by the modules is only 1°C more that NOCT value, which is 47°C at 20°C air temperature, 800 W/m^2 irradiance, and 1 m/s wind speed. This can be put down to a wind speed between 2 and 5 m/s during the experiments.

The following recommendations are given taking into account our experience about outdoor measurements in addition to the requirements listed in,[10,35] and.[36] The following actions have been performed during the measurements campaign:

- If the irradiance received by the PV module is $G > 1{,}000$ W/m^2, which is quite usual in summer in Málaga, the orientation of the tracker is changed in order to have a G value as much close to G_{STC} as possible.
- A thermo-electric pyranometer has been mounted close to the PV module and with a difference between their orientations that is smaller than ±2°. This allows to have an accurate measurement of the irradiance level the PV module actually works at.
- A second irradiance sensor, having a time response that is shorter than the one of the pyranometer, has been also installed on the same plane of the PV module. This sensor is able to keep track of rapid changes of the irradiance level the PV module should be subjected to that are out of the pyranometer bandwidth.[37] For the experimental measurements presented in this paper, a calibrated cell of the same technology of the modules has been used. It must be taken into account that the irradiance level associated to the

measurements will be the reported by the pyranometer, while the reading from the reference cell will be only used to perform a correction procedure.

- The *I*–*V* curve has to be acquired in a time interval that is significantly shorter than the one *G* needs for changing more than 1% of its value. The irradiance level is measured before and after the acquisition of the *I*–*V* curve, so that only the curves characterized by an irradiance difference equal to 5 W/m^2 are considered.
- The stepper motor solar tracker updates its orientation regularly, for example, every minute. This operation is paused during the acquisition of the *I*–*V* curves, in order to eliminate a source of variation of *G* during the measurements.
- Ideally, measurements should be performed under a perfectly clear sky. Unfortunately, that condition is rarely available, due to some small and thin clouds, mist, or smoke. The *I*–*V* curves have been acquired within an interval of 2 h centered on the solar noon, so that a negligible variation of G is obtained. Measurements used in this paper refer to $G \in [980, 1{,}020]$ W/m^2.
- The wind speed during the experiment has been recorded. In theory, only measurements corresponding to a wind speed lower than 2 m/s should be considered. Nevertheless, by considering the climate characteristics of Málaga, a wind speed threshold at 4 m/s has been settled.
- As in a real PV module each cell works at a temperature value that might be slightly different from the others,[5] the temperature value used in the regression procedure has been computed as the average of the output of four Pt100 RTD sensors. The cells close to the junction box should be avoided. It is useful to put the PV module in short-circuit and then use a thermographic camera for selecting working at a temperature that is the average of the range of temperatures reached by the module cells.
- The PV module temperature is measured by adhering the four sensors to its back surface. Each sensor is placed at the center of the selected cell. Thermal paste has been used between the surface of the sensors and the back layer of the module, in order to improve the heat transfer. In addition, aluminum adhesive tape has also been used to fix the sensors.
- The current-voltage points of each *I*–*V* curve are recorded by using high-resolution multimeters, that is, Agilent 34410A with $6\frac{1}{2}$ digits. The higher the resolution, the greater the integration time and the smaller the maximum number of acquired points. The measurements used in this paper have been acquired with a resolution of $6\frac{1}{2}$ digit, so that each *I*–*V* curve including 150 samples is acquired in 1 s.

4.2 | Selection of the temperature range

Depending on the season of the year and the climatic conditions of the installation where the measurements are performed, the temperature range taken into account in the linear regression should be different. Therefore, this range cannot be predefined in general but some recommendations are given from our experience. The minimum bound depends on the minimum temperature that it is possible to achieve using the cooling method used; in our case (Málaga in summer and clear-sky days) it is around 22–23°C. However, to this value, we must add an offset for the reason that we will explain in the following. Figure 2 shows the V_{OC} versus *T* measured on the back surface of the PV module. The trend appears to be non-linear at low temperatures, thus between 23°C and 28°C. This weird behavior is due to the fact that the encapsulating materials between the cells and the sensor on the back surface cause a delay.

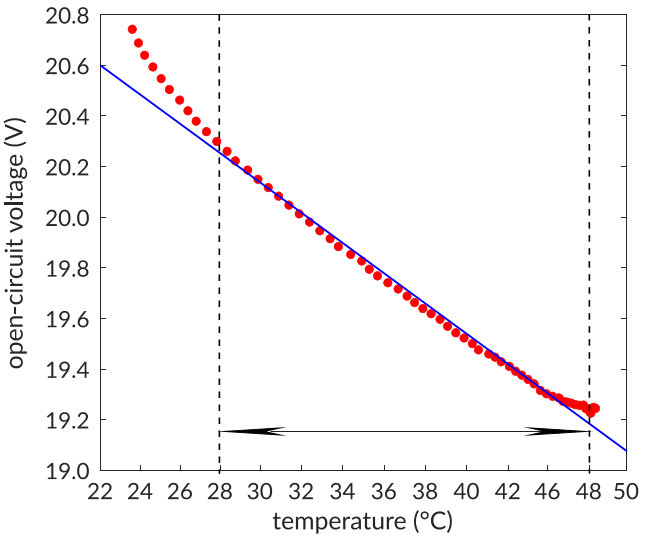

FIGURE 2 Open-circuit voltage V_{OC} versus module temperature *T* over all the range [Colour figure can be viewed at wileyonlinelibrary.com]

In general, it is not easy to measure the actual cell temperature, assuming as cell temperature the value obtained from the sensors on back surface. The discrepancy is very high at the beginning obtaining erroneous values for the temperature coefficients, but after 28°C, we have assumed that the difference will remain almost stable. In general, it is assumed that this discrepancy is 2.5°C ± 1°C, [38] implying that each measurement should be corrected by a fixed increment of 2.5°C and a standard deviation of $\left(1/\sqrt{3}\right)^{\circ}$ C. However, in this work, a small cut in the back layer of one of the modules under study was done to install an internal Pt100 sensor (removing the silicone sheath) in direct contact to the cell, in order to compare its readings with the measurement of another external Pt100 sensor attached to the back layer. During 2 h before and 2 h after the solar noon of a perfect clear-sky day, at regular intervals of 1 s, a set of measurements of both Pt100 (internal and external) have been stored and the difference between both readings has been computed. In our case, the mean value of all these differences was exactly 2.5°C and the associated standard deviation from this mean value was 0.52°C.

Just after uncovering the module, the cell temperature starts to rise immediately; as a consequence, V_{OC} decreases at the same rate. However, this change cannot be detected by the sensor on the back surface until a time due to slow thermal response of the back layers, so that the real behavior appears to be distorted. As time goes by, thus, as the cell temperature increases, the sensor reacts and, although it measures a temperature that is lower than the real one, the rate of increment is preserved. This occurs approximately after that the temperature measured by the back surface RTD has become higher than the initial one by 5°C. As a consequence, only those

measurements referring to a PV module temperature higher than 28°C have been the ones used to evaluate the temperature coefficients in this work.

After some minutes from the beginning of the experiment, the temperature tends to its stationary value, thus fluctuating around it. The closer the stationary value, the smaller the temperature increase between two consecutive measurements. Also the *I*–*V* curves acquired in this time interval have not been considered in the linear regression aimed at calculating the temperature coefficients. Including these measurements should give an excessive number of points at the end of the regression line, thus influencing badly the computed values. In the performed experiments, the temperature reaches a stationary value around 48°C. In conclusion, the linear regressions used for determining the temperature coefficients have been performed within the temperature range. As it has been said above, this interval will depend on the emplacement and the season of the year, so if the procedure will be applied on other site or season, a different interval should be considered.

Figure 2 shows a slightly non-linear relationship between the open-circuit voltage and the cell temperature. Although the cloud of points deviates in a systematic way from a straight line, it appears that a linear trend gives a reasonably accurate approximation of the phenomenon in the central range of temperatures.

4.3 | Calculation of the main electrical parameters

The numerical values of I_{SC}, V_{OC}, P_{max}, I_{Pmax}, and V_{Pmax} are computed from the discrete measured points of each *I*–*V* curve.[39] If I^*_{SC} is the current value of the point closer to the $V = 0$ axis and V^*_{OC} the voltage value of the point closer to the $I = 0$ axis, it is possible to select all the points inside **BOX–1** (red) in Figure 3 and defined by (Equation 1):

$$[0\text{V}, 20\%V^*_{OC}] \times [I^*_{SC} - 4\%I^*_{SC}, I^*_{SC} + 4\%I^*_{SC}] \quad (1)$$

Afterwards, a least mean square (LMS) *linear regression* is used to determine I_{SC}. The selected voltage interval excludes samples having a negative voltage value, because the non-linear behavior due to the bypass diodes might affect the regression. The estimation of V_{OC} is performed in a similar way. The *I*–*V* points to interpolate are those ones falling within **BOX–2** (cyan) in Figure 3 according to (Equation 2):

$$[V^*_{OC} - 10\%V^*_{OC}, V^*_{OC} + 10\%V^*_{OC}] \times [-20\%I_{SC}, +20\%I_{SC}] \quad (2)$$

The value V_{OC} is then evaluated. In order to calculate the maximum power point, first a rough approximation P^*_{max} is taken as the maximum value from all the products $V_i \times I_i$ of the discrete points of the *I*–*V* curve. Hence, all the points whose power fall within the following interval (**BOX–3**, green color, in Figure 3) are considered (Equation 3):

$$[85\%P^*_{max}, 100\%P^*_{max}] \quad (3)$$

Finally, a *fifth-degree* polynomial is fitted using an LMS regression and the first derivative of that polynomial is fixed to be equal to zero.[40] Among all the roots, the real one falling in the voltage range of the selected points is considered, so that V_{Pmax}, I_{Pmax}, and P_{max} are determined.

4.4 | Estimation of the temperature coefficients

Aimed at evaluating the partial derivative of the open-circuit voltage with respect to the PV module temperature, the V_{OC} value is measured at different temperature values, by acquiring *I*–*V* curves corresponding to a narrow range of irradiance level, between 980 and 1,020 W/m^2. Once the value read by the pyranometer falls within this range, the cover on the PV module is removed, so that it is exposed to the sun radiation, and the measurement system starts the repeated acquisition of the *I*–*V* curves. As the PV module heats up, the acquired *I*–*V* curves correspond to increasing temperature values, from a minimum value up to the thermal stationary state. Any *I*–*V* curve corresponding to an irradiance value outside the specified range is discarded. The V_{OC} is computed for each measured *I*–*V* curve, so that a plot of V_{OC} vs *T* is done. Figure 4(left) and Figure 4(right) refer to the modules **1** and **2** (see summary in Table 2). The slope resulting from the fitting of this plot is β. Due to the significant influence of *T* on V_{OC}, the coefficient of determination R^2 of the regression is very close to 1. The result shown in Figure 4(right) is slightly worse in terms of R^2 because the experiment was performed on a day with higher values

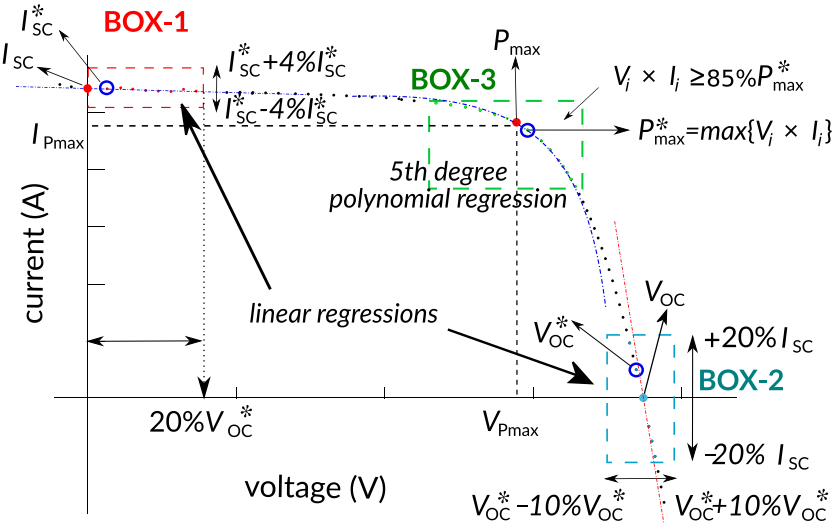

FIGURE 3 Estimation of I_{SC}, V_{OC}, P_{max}, I_{Pmax}, and V_{Pmax} [Colour figure can be viewed at wileyonlinelibrary.com]

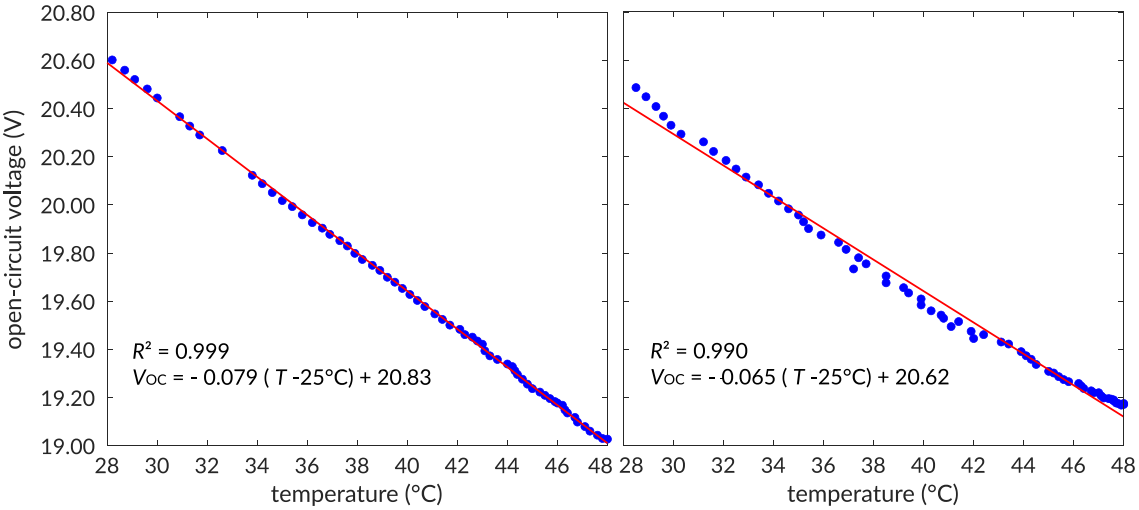

FIGURE 4 Estimation of β for module **1** (left) and module **2** (right) [Colour figure can be viewed at wileyonlinelibrary.com]

TABLE 2 Estimation of α, β, and δ and their respective standard uncertainties

#	Serial number	$\beta \pm u_\beta$ mV/°C	R^2	$\alpha \pm u_\alpha$ mA/°C	R^2	$\delta \pm u_\delta$ mW/°C	R^2
-	**I-53**	**−80**		**+1.29**		**−256**	
1	946307	−79 ± 5	0.999	+0.96 ± 0.22	0.853	−181 ± 22	0.997
2	946406	−65 ± 4	0.990	+0.89 ± 0.19	0.929	−150 ± 18	0.987
3	946412	−64 ± 4	0.995	+0.92 ± 0.18	0.953	−161 ± 19	0.993
4	946418	−61 ± 5	0.989	+1.02 ± 0.25	0.819	−144 ± 21	0.975
5	946410	−70 ± 5	0.993	+0.92 ± 0.23	0.762	−165 ± 22	0.985
6	946425	−68 ± 5	0.998	+0.98 ± 0.22	0.904	−149 ± 20	0.997
7	946303	−74 ± 5	0.996	+0.87 ± 0.21	0.908	−188 ± 24	0.997
8	946431	−79 ± 7	0.999	+1.07 ± 0.34	0.799	−186 ± 32	0.992
9	946430	−76 ± 6	0.998	+0.92 ± 0.26	0.745	−206 ± 28	0.994
–	**mean**	**−71 ± 5**		**+0.95 ± 0.23**		**−170 ± 23**	
–	**SD.abs**	**7**		**0.06**		**21**	
–	**SD.rel**	**9%**		**7%**		**13%**	

of wind speed: a mean value of 1.5 m/s during the measurements for the module **1** versus 3.0 m/s during the test of the module **2**. The open-circuit voltage $V_{OC,STC}$ at STC is obtained by looking at the value of the regression line at $T = 25°$ C that is the independent term of the equation of the line. For instance, Figure 4 shows that the $V_{OC,STC}$ of the modules **1** and **2** are 20.83 and 20.62 V, respectively. Although all the modules are nominally of the same model, after 21 years of operation, their temperature coefficients could have changed in a different way, depending on how each one has degraded.

Unlike V_{OC}, the short-circuit current I_{SC} depends primarily on the incident irradiance G, being the influence of the module temperature a second-order factor. The measurement of the correlation between I_{SC} and T is quite involved because the changes of the current due to the temperature variation are small in comparison to those due to irradiance. Even in a perfect clear-sky day, the fast and small oscillations of the irradiance level produce changes in I_{SC} that mask the change due to temperature. To overcome this problem, Carlsson et al.[41] propose to perform the linear regression over I_{SC}/G instead of I_{SC}, where G is the irradiance measured by a reference cell of equivalent technology. A similar correction procedure is proposed in this paper. For each I–V curve, in addition to the reading of the pyranometer, the short-circuit current $I_{SC,ref}$ of the reference cell is also registered. The temperature of this cell remains stable because it is installed permanently on the solar tracker, and it has not been uncovered or cooled down before the measuring process. Thus, the corrected short-circuit current $I_{SC,corr}(t_i)$ acquired at a time instant t_i is calculated from the estimated $I_{SC}(t_i)$, by applying (Equation 4):

$$I_{SC,corr}(t_i) \approx I_{SC}(t_i) \cdot \frac{\overline{I_{SC,ref}}}{I_{SC,ref}(t_i)} \tag{4}$$

where $I_{SC,ref}(t_i)$ is the short-circuit current of the reference cell at that time t_i and $\overline{I_{SC,ref}}$ is the mean value of all the readings of the reference cell during the same experiment.

In Figure 5(left), the behavior of the I_{SC} with respect to T for the module **3** is shown. A linear correlation that fits the measured values is almost unrecognizable. It is clearly seen that there is a waveform oscillation due to the irradiance variation superposed to the trend caused by the temperature increment. However, by applying the correction procedure explained above, the result shown in Figure 5(right) is obtained. Then, the slope of the line is a good approximation of α, with $R^2 = 0.953$. The proposed correction method allows to cancel out the effect of the variation of G, because this effect appears in the numerator and in the denominator of (Equation 4). It is not possible to accomplish the proposed correction using the irradiance readings from a thermo-electric pyranometer because its response time is too

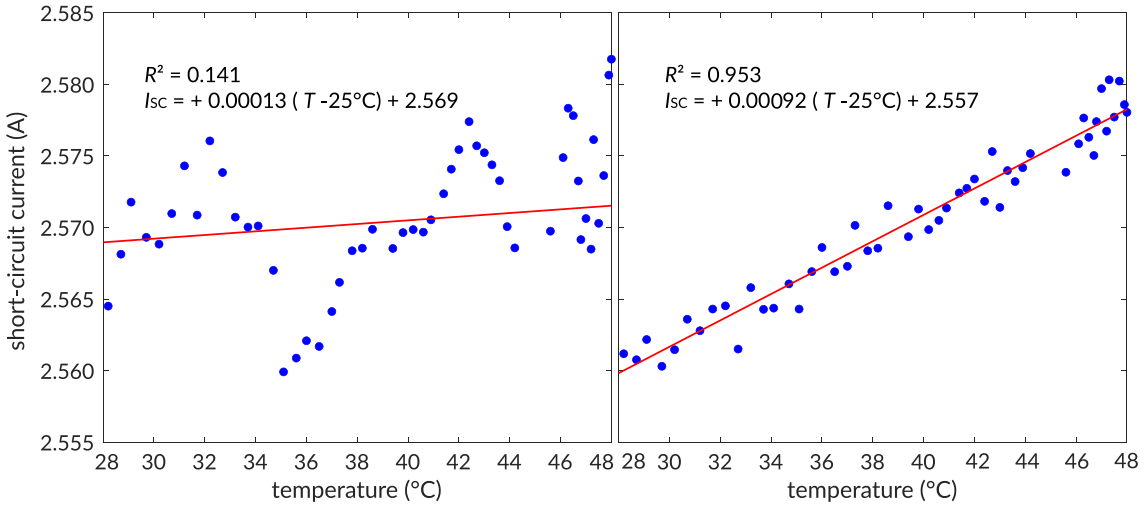

FIGURE 5 Estimation of α for module **3** before correction (left) and after correction (right) [Colour figure can be viewed at wileyonlinelibrary.com]

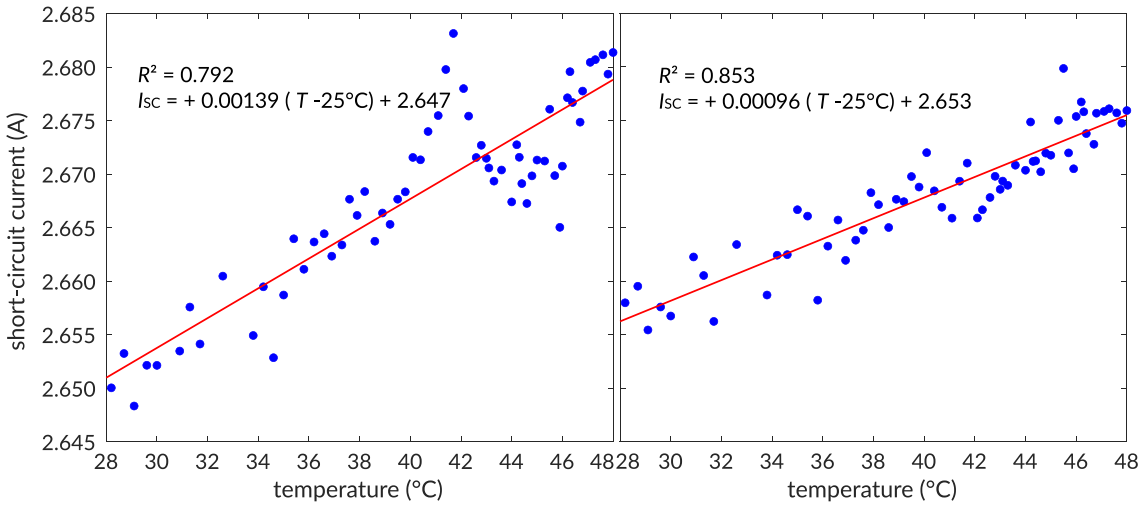

FIGURE 6 Estimation of α for module **1** before (left) and after correction (right) [Colour figure can be viewed at wileyonlinelibrary.com]

slow to detect the fast G changes that have a non-negligible effect on the PV module current.[37] The value that the fitting line assumes at $T = 25°C$ is the $I_{SC,STC}$ corresponding o the module **3**: it is approximately 2.557 A. This calculus can be done for every PV module under study.

During some of the experiments, a gradual increase of G that reinforces the rise of I_{SC} due to T has been noted. This leads to an acceptable R^2, but, unfortunately, to an inaccurate estimated value of α, because of the combined effect of G and T. This can be seen for the module **1** in Figure 6: before applying the correction (left), a value $\alpha = 1.39$ mA/°C is obtained with an R^2 of 0.792. After applying the correction formula (right), we achieve $\alpha = 0.96$ mA/°C with a better R^2 value. Although 1.39 mA/°C is closer to the nominal value, after 21 years of operation, a decrement of α is expected. In order to ensure an uniform analysis, the correction procedure has been applied in every case.

In order to determine δ, it could be taken into account that the maximum power P_{max} of the PV module depends on I_{SC} and V_{OC}. As in the case of α, it would be possible to apply some kind of correction procedure to cancel the influence of the irradiance fluctuation on the maximum power value. However, in this work no correction procedure has been applied to P_{max}. The coefficient of determination R^2 is recommended to be used as an indicator to decide if the experiment should or not be repeated (in this paper a minimum R^2 of 0.7 has been considered). However, a good value of R^2 is not enough to ensure the reliability of the obtained results. In fact, the obtained results could be validated using α, β, and δ to correct the electrical parameters of a test set of curves to STC and analyze the standard deviation of the translated parameters. Again, for each specimen, it is possible to estimate $P_{textrmmax,STC}$ as the interception of the regression line to $T = 25°C$. As it can be seen in Figure 7, in case of module **2** it is 38.0 W and for module **3** it is 38.5 W.

4.5 | Analysis of uncertainty

Following the approach described by Whitfield and Osterwald,[38] it is possible to calculate the uncertainty associated to each individual voltage measurement of the I–V curve, assuming a voltmeter Agilent 34411A[42] (operating at ±100 V range, A/D converter of 21 bit and 300 readings/s). A second Agilent voltmeter of the same type has been used for an individual measurement of current, obtained by

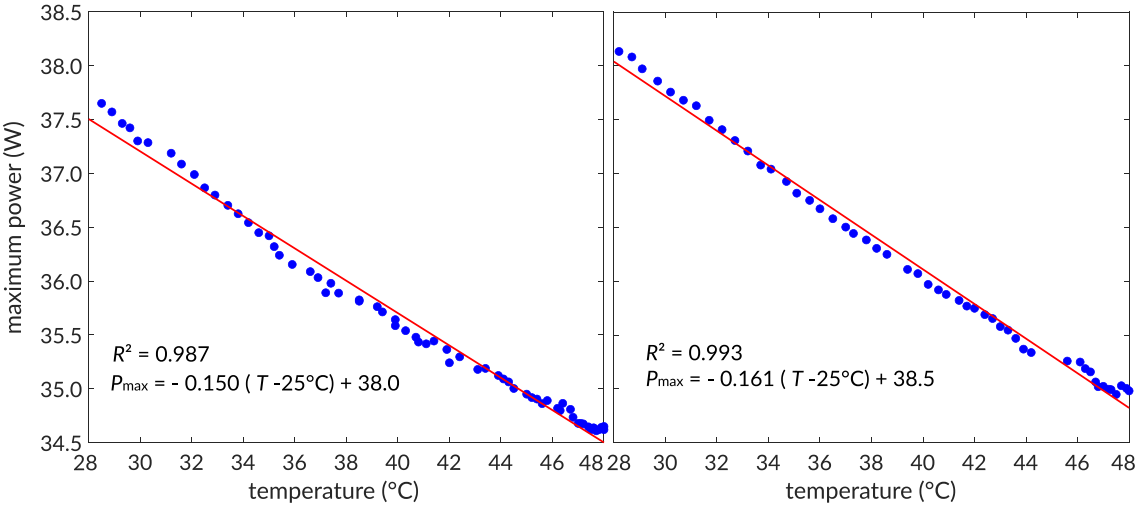

FIGURE 7 Estimation of δ for module **2** (left) and module **3** (right) [Colour figure can be viewed at wileyonlinelibrary.com]

sensing the voltage drop across a calibrated resistor (of certified class 0.1) in series between the PV module and power supply (see[33]), by settling the voltage range to ±100 mV. In both cases a span of 1 year since the last calibration has been assumed with a TUR (tolerance to uncertainty ratio) of 4:1, and no temperature drift has been applied. This leads to (Equation 5) and (Equation 6) for estimating the standard uncertainties u_V and u_I, respectively. Then, using the propagation rule of uncertainty given in ISO/IEC Guide 98-3[43] over the expression $P = I \cdot V$, the standard uncertainty u_P is associated to an individual value of power estimated using (Equation 7).

$$u_V = \left(5.6e-10 \cdot V^2 + 5.9e-8 \cdot V + 1.5e-6\right)^{1/2} \tag{5}$$

$$u_I = \left(3.3e-7 \cdot I^2 + 6.5e-8 \cdot I + 1.2e-6\right)^{1/2} \tag{6}$$

$$u_P = \left(3.3e\text{-}7I^2V^2 + 5.9e\text{-}8I^2V + 1.5e\text{-}6I^2 + 6.5e\text{-}8V^2I + 1.2e\text{-}6V^2\right)^{1/2} \tag{7}$$

For each I–V curve, in addition to the main electrical parameters (I_{SC}, V_{OC}, and P_{max}), their standard uncertainties ($u_{I_{SC}}$, $u_{V_{OC}}$, and $u_{P_{max}}$ respectively) should be computed, taking into account how the initial uncertainties of the interpolating points are propagated to the final result. In the case of I_{SC} or V_{OC}, the expressions provided by York et al.[44] to propagate the error have been used. The implementation for Matlab coded by Wiens[45] provides the best line in addition to the associated uncertainties of the slope and the intercept (the error of the estimated electrical parameter), using as input a set of I–V points with uncertainty in the both axes. However, the estimation P_{max} requires a more complex procedure and it is very difficult to obtain expressions to propagate the error from the initial data; so it is common to address this type of problem through the Monte Carlo method,[46] implemented in Matlab by Robens,[47] that allows to simulate the fitting procedure for each I–V curve, returning an estimation for $u_{P_{max}}$.

Accordingly to Whitfield and Osterwald,[38] the standard uncertainty u_T due to the measurement of the PV module temperature is estimated combining several sources of uncertainty, such as the resolution of the thermometer, its reported accuracy, and the uncertainty of the reference calibrator, as it can be seen in Equation (8). In our case, the manual of the module cFP-RTD-124[48] (used to measure the four RTD Pt100 sensors) reports a maximum error of $e_T = 0.25°$ C in the temperature range of interest and a measurement range of (−200,+850)°C using an A/D converter of $n = 16$ bit (a TUR of 4:1 is assumed). However, the largest contributor by far to the uncertainty is related to the difference between the actual junction cell temperature and the back surface temperature. As it is explained in Section 4.2, instead of using the generic approximation given in the previous literature $\left(2.5 \pm 1/\sqrt{3}°C\right)$, the correction to apply in this work and its associated uncertainty have been estimated for this model of PV module as (2.5 ± 0.52°C). The final value for the uncertainty u_T (for the studied temperature range) is 0.54°C:

$$\begin{aligned} u_T &= \left(\left(\frac{T_{max} - T_{min}}{2^n \cdot \sqrt{12}}\right)^2 + \left(\frac{e_T}{\sqrt{3}}\right)^2 + \left(\frac{e_T}{2 \cdot 4}\right)^2 + (u_\Delta)^2\right)^{1/2} \\ &= \left(\left(\frac{1050}{2^{16} \cdot \sqrt{12}}\right)^2 + \left(\frac{0.25}{\sqrt{3}}\right)^2 + \left(\frac{0.25}{2 \cdot 4}\right)^2 + (0.52)^2\right)^{1/2} \end{aligned} \tag{8}$$

Before estimating the temperature coefficients, the value $I_{SC,corr}$ is obtained using (Equation 4), so that this correction procedure also propagates the standard uncertainties of its input variables, following (Equation 9) and (Equation 10):

$$u_{\overline{I_{SC,ref}}} = \frac{1}{N}\sqrt{\sum_{i=1}^{N}\left[u_{I_{SC,ref}}(t_i)\right]^2} \tag{9}$$

$$u_{I_{SC,corr}}(t_i) = \sqrt{\begin{aligned} &\left(\frac{\overline{I_{SC,ref}}}{I_{SC,ref}(t_i)} \cdot u_{I_{SC}}(t_i)\right)^2 + \\ &\left(\frac{I_{SC}(t_i)}{I_{SC,ref}(t_i)} \cdot u_{\overline{I_{SC,ref}}}\right)^2 + \\ &\left(\frac{\overline{I_{SC,ref}} \cdot I_{SC}(t_i)}{[I_{SC,ref}(t_i)]^2} \cdot u_{I_{SC,ref}}(t_i)\right)^2 \end{aligned}} \tag{10}$$

where N is the number of curves of each experiment. The uncertainty $u_{I_{SC,ref}}$ at time t_i is estimated according to Müllejans et al.,[49] combining several sources of error (orientation and alignment, spectral mismatch, calibration drift …), but only those that could change during the same experiment are taken into account in this paper: the resolution of the acquisition system, its reported accuracy, and the variability of the

reference cell temperature during the experiment (before combining, this value is converted from °C to A multiplying it by the current temperature coefficient of the reference cell $\alpha^* = 0.00129$ A/°C, assuming in this case the nominal value because the reference cell used has been working for a negligible time before being used in the experiments described in this paper). Assuming a module cFP-AI-112[50] with a range of ±300 mV and an A/D converter of 16 bit, (Equation 11) is obtained to estimate $u_{I_{SC,ref}}$, where $u_{T_{ref}}$ is the standard deviation of all the measurements of the reference cell temperature (measured using an extra Pt100 sensor):

$$u_{I_{SC,ref}}(t_i) = \Big(3.0e-8 \cdot I^2_{SC,ref}(t_i) + 2.4e-7 \cdot I_{SC,ref}(t_i) + 1.7e-6 \cdot u^2_{T_{ref}} + 4.8e-7\Big)^{1/2} \quad (11)$$

Finally, when the temperature coefficients α, β, and δ are computed, their respective uncertainties should also be estimated. The linear regression procedures to be applied must take into account that the input points are affected by uncertainty in both axes, so the equations of propagation given by York et al.[44] are again applicable to obtain the values of u_α, $u_{\beta,}$ and u_δ.

5 | RESULTS AND DISCUSSION

Table 2 summarizes the estimations of the temperature coefficients for the main electrical parameters in addition to their respective uncertainties.

The coefficients of determination R^2 associated to the linear regressions procedures have also been included. The first row shows the nominal or reference values provided by the manufacturer for each coefficient. The last three rows, in bold, give the mean values over the nine modules and the standard deviation (absolute and relative), respectively. The first two columns are used to identify each PV module tested. The β values vary in a range from −79 to −61 mV/°C, with a mean of −71 mV/°C and a standard deviation of 7 mV/°C (around 9%). On average, the absolute value of this coefficient is slightly higher than the value measured by TÜV Rheinland for a new module (−80 mV/°C). In addition, by referring to a single cell, a value $\beta_{cell} \approx -1.97$ mV/°C is obtained, which is a bit lower than the experimental results that are published.[22,26,51] It should be noted that the estimations of β are achieved with high values of R^2, quite close to one. Moreover, the value of the standard deviation of β among all the modules is close to the values of uncertainty of β of each PV module.

The temperature coefficient α assumes values ranging from $+0.87 to + 1.07$ mA/°C with an average equal to +0.95 mA/°C. By taking into account the estimated uncertainties, the latter value is in agreement with the value alpha measured by TÜV Rheinland by using a solar simulator for a new module, which is +1.29 mA/°C. Indeed, the decrement of α is a direct consequence of the decrement of I_{SC} due to the degradation of the modules, which have been under operation for more than 21 years.King et al.[8] state that the value of α at STC must be scaled to be used at a different irradiance level that G_{STC}. For the same reason, if I_{SC} decreases due to the effect of degradation, then it is expected that α will also decrease as time goes by. Finally, to be honest, we should highlight the huge values of uncertainty associated to the reported values of α, taking into account that these are standard uncertainties (coverage factor $k = 1$). However, very high uncertainties in this temperature coefficient are also reported in previous literature.[14,52]

The correction procedure to obtain $I_{SC,corr}$ removes the main contribution from G but does not push the values R^2 obtained in the linear regressions very close to 1. Indeed, for some modules, the R^2 values are between 0.8 and 0.9 (even more), but for some others they are close to 0.7. This result highlights the difficulty of experimentally measuring this parameter under outdoor conditions.

The values of the temperature coefficient δ range from −206 to −144 mW/°C. The mean value is −170 mW/°C, and the standard deviation is 21 mW/°C (around 13%). The R^2 values are a bit lower than the ones for β. The value of δ for a new module is −256 mW/°C, quite far from the identified values for the degraded modules. As with α, this discrepancy might be due to the degradation of the modules. But it is also true that the reference value is estimated by using indoor laboratory measurements. Also, very high values of standard uncertainty type B have been estimated for δ. It must be taken into account that we are not only referring to direct measurements but

TABLE 3 Estimation of α_{rel}, β_{rel}, and δ_{rel} with their respective uncertainties

#	Serial number	$V_{OC,STC}$ V	$\beta_{rel} \pm u_\beta$ %/°C	$I_{SC,STC}$ A	$\alpha_{rel} \pm u_\alpha$ %/°C	$P_{max,STC}$ W	$\delta_{rel} \pm u_\delta$ %/°C
-	**I-53**		**−0.37**		**+0.039**		**−0.48**
1	946307	20.83	−0.38 ± 0.02	2.653	+0.036 ± 0.008	39.6	−0.47 ± 0.06
2	946406	20.62	−0.32 ± 0.02	2.594	+0.034 ± 0.007	38.0	−0.39 ± 0.05
3	946412	20.65	−0.31 ± 0.02	2.557	+0.036 ± 0.007	38.5	−0.39 ± 0.05
4	946418	20.50	−0.30 ± 0.02	2.564	+0.040 ± 0.010	37.4	−0.38 ± 0.06
5	946410	20.66	−0.34 ± 0.02	2.610	+0.035 ± 0.009	38.2	−0.42 ± 0.06
6	946425	20.51	−0.33 ± 0.02	2.609	+0.038 ± 0.008	37.7	−0.41 ± 0.05
7	946303	20.68	−0.36 ± 0.02	2.611	+0.033 ± 0.008	38.9	−0.45 ± 0.06
8	946431	20.69	−0.38 ± 0.03	2.573	+0.042 ± 0.013	38.7	−0.48 ± 0.08
9	946430	20.78	−0.37 ± 0.03	2.657	+0.035 ± 0.010	39.9	−0.44 ± 0.07
–	**mean**	**20.66**	**−0.34 ± 0.02**	**2.603**	**+0.036 ± 0.009**	**38.5**	**−0.43 ± 0.06**
–	**SD.abs**	**0.11**	**0.03**	**0.036**	**0.003**	**0.8**	**0.04**
–	**SD.rel**	**0.5%**	**9%**	**1.4%**	**7%**	**2.2%**	**8%**

Note. Bold emphasis in the third row contains the nominal parameters (from the specification sheet) of the studied photovoltaic modules while the three last rows contain summarized values (mean and standard deviation) among all the studied photovoltaic modules under study.

also to values computed by a sequence of several algorithms, in such a way multiple sources of uncertainty are combined.

As the independent term of each regression line provides an estimation of $V_{OC,STC}$, $I_{SC,STC}$, or $P_{max,STC}$ for the modules from **1** to **9** (see Table 3), it is possible to calculate the relative values β_{rel}, α_{rel}, and δ_{rel} in STC for each degraded PV module under test. In addition, the relative temperature coefficients for a new PV module can be calculated from the specification sheet, obtaining nominal values of $\beta^*_{rel} = -0.37\%/^\circ$ C, $\alpha^*_{rel} = +0.039\%/^\circ$ C, and $\delta^*_{rel} = -0.48\%/^\circ$ C. They have been listed on the top of Table 3.

These standardized temperature coefficients do not depend on specific features of the Isofotón I–53, for example, the number of cells, so that they are useful for a comparison with the literature values.[7] The obtained mean value of $\beta_{rel} = -0.34 \pm 0.02\%/^\circ$C is close to the nominal one β^*_{rel} and also to those ones reported in all the literature referring to sc-Si devices.[8,9,24,25,53-55] By taking into account the estimation of $I_{SC,STC}$ (see Table 3), the mean value of $\alpha_{rel} = +0.036 \pm 0.09\%/^\circ$C can be compared with the nominal one and some other values published in literature, regardless of the cell area and of the number of strings in parallel within the PV module. Values previously reported[9,25,53,56] are in agreement with those ones obtained through the procedure proposed in this paper. It has to be kept into account that the calculation of this coefficient is affected by a high number of factors and sources of uncertainty.[12] Finally, in order to compare the maximum power temperature coefficient to other reported values, the mean value $\delta_{rel} = -0.43 \pm 0.06\%/^\circ$C is considered. The obtained result is in agreement again with the nominal one and others published in literature and referring to sc-Si cells.[14,26,29,31,51,57]

6 | CONCLUSIONS AND FUTURE RESEARCH

In this paper a comprehensive and detailed step by step guide to determine the temperature coefficients of commercial PV modules through experimental measurements acquired outdoors is described. In this way, the values of β, α, and δ are estimated under outdoor real operating conditions. The published literature lacks studies such as the work presented in this paper although the topic is an important matter because the temperature coefficients are necessary to characterize the electrical behavior of a PV module and consequently to forecast its energy yield. The proposed procedure has been applied successfully to nine commercial PV modules; linear regressions of the experimental data have been performed with high R^2 values. The results presented in the paper show that this goal has especially been achieved for β and δ, with coefficients of determination that are very close to 1. A lower R^2 value has been obtained for the coefficient α, but the improvement achieved through the proposed correction procedure is shown to be significant.

The relationship between the ageing of the PV modules after 21 years of exposure and the temperature coefficients has also been addressed. From the results, we can conclude that the absolute values of α and δ have been decreased significantly as a consequence of the degradation. However, in terms of the normalized temperature coefficients (α_{rel}, β_{rel}, and δ_{rel}) and taking into account the uncertainty in the determination of those values, nothing can be concluded, because the observed variation is less than the uncertainty.

Further work should address the effects of the temperature on other parameters of the PV module, for example, on the series and shunt resistance or on the diode ideality factor. The application of the proposed procedure to other technologies, having a different parameters correlations with the temperature, would also be of great interest.

ACKNOWLEDGEMENT

This work has been supported by the project RTI2018-095097-B-I00 at the 2018 call for I+D+i Project of the Ministerio de Ciencia, Innovación y Universidades, Spain.

ORCID

M. Piliougine https://orcid.org/0000-0002-8169-9727
M. Sidrach-de-Cardona https://orcid.org/0000-0002-7030-4232
G. Spagnuolo https://orcid.org/0000-0002-4817-1138

REFERENCES

1. Prince MB. Silicon solar energy converters. *J Appl Phys*. 1955;26(5):534-540. https://doi.org/10.1063/1.1722034
2. Wysocki JJ, Rappaport P. Effect of temperature on photovoltaic solar energy conversion. *J Appl Phys*. 1960;31(3):571-578. https://doi.org/10.1063/1.1735630
3. Patterson RE, Yasui RK. Parametric performance characteristics and treatment of temperature coefficients of silicon solar cells for space application. No. JPL-TR-32-1582, Pasadena (CA, USA): Jet Propulsion Laboratory (NASA), California Institute of Technology, https://ntrs.nasa.gov/search.jsp?R=19730015363; 1973.
4. Hovel HJ. Chapter 8—Temperature and intensity. In: Willardson RK, Beer AC, eds. *Solar Cells*, Vol. 11. New York (NY USA): AC Academic Press. of Semiconductors and semimetals; 1975:166-180. https://doi.org/10.1016/S0080-8784(08)62349-2
5. Osterwald CR. Chapter III-2—Standards calibration, and testing of PV modules and solar cells. In: McEvoy A, Markvart T, Castañer L, eds. *Practical Handbook of Photovoltaics*. 2ed. Boston (MA, USA): Academic Press; 2012:1045-1069. https://doi.org/10.1016/B978-0-12-385934-1.00034-9
6. Osterwald CR, Glatfelter T, Burdick J. Comparison of the temperature coefficients of the basic I–V parameters for various types of solar cells. In: 19th IEEE Photovoltaic Specialists Conference PVSC New Orleans (LA, USA); 1987:188-193. https://www.nrel.gov/docs/legosti/old/9061.pdf
7. Emery K, Burdick J, Caiyem Y, Dunlavy D, Field H, Kroposki B, et al. Temperature dependence of photovoltaic cells, modules and systems. In: 25th IEEE Photovoltaic Specialists Conference PVSC; 1996:1275-1278. https://doi.org/10.1109/PVSC.1996.564365
8. King DL, Kratochvil JA, Boyson WE. Temperature coefficients for PV modules and arrays: Measurement methods, difficulties, and results. In: 26th IEEE Photovoltaic Specialists Conference PVSC; 1997:1183-1186. https://doi.org/10.1109/PVSC.1997.654300
9. Fanney AH, Davis MW, Dougherty BP, King DL, Boyson WE, Kratochvil JA. Comparison of photovoltaic module performance measurements. *J Sol Energy Eng*. 2006;128(2):152-159. https://doi.org/10.1115/1.2192559
10. IEC 60891. Photovoltaic devices—Procedures for temperature and irradiance corrections to measured I–V characteristics. 2 ed. Geneva

(Switzerland): International Electrotechnical Commission IEC, https://webstore.iec.ch/publication/3821; 2009.
11. Dupré O, Vaillon R, Green MA. Physics of the temperature coefficients of solar cells. *Sol Energ Mat Sol C*. 2015;140:92-100. https://doi.org/10.1016/j.solmat.2015.03.025
12. Osterwald CR, Campanelli M, Kelly GJ, Williams R. On the reliability of photovoltaic short-circuit current temperature coefficient measurements. In: 42nd IEEE Photovoltaic Specialist Conference PVSC New Orleans. LA USA; 2015:1-6. https://doi.org/10.1109/PVSC.2015.7355842
13. Hishikawa Y, Yoshita M, Ohshima H, Yamagoe K, Shimura H, Sasaki A, et al. Temperature dependence of the short circuit current and spectral responsivity of various kinds of crystalline silicon photovoltaic devices. *Jpn J Appl Phys*. 2018;57(8S3):08RG17. https://doi.org/10.7567/jjap.57.08rg17
14. Salis E, Pavanello D, Trentadue G, Müllejans H. Uncertainty budget assessment of temperature coefficient measurements performed via intra-laboratory comparison between various facilities for PV device calibration. *Sol Energy*. 2018;170:293-300. https://doi.org/10.1016/j.solener.2018.04.062
15. Sandstrom JD. A method for predicting solar cell current–voltage curve characteristics as a function of incident solar intensity and cell temperature. No. JPL-TR-32-1142, Pasadena (CA, USA): Jet Propulsion Laboratory (NASA), California Institute of Technology, https://ntrs.nasa.gov/search.jsp?R=19670021539; 1967.
16. IEC 60904–10. Photovoltaic devices—Part 10: Methods of linear dependence and linearity measurements. 3 ed. Geneva (Switzerland): International Electrotechnical Commission IEC, https://webstore.iec.ch/publication/60066; 2020.
17. IEC 60904–9. Photovoltaic devices—Part 9: Classification of solar simulator characteristics. 3 ed. Geneva (Switzerland): International Electrotechnical Commission IEC, https://webstore.iec.ch/publication/28973; 2020.
18. IEC 60904–3. Photovoltaic devices—Part 3: Measurement principles for terrestrial photovoltaic (PV) solar devices with reference spectral irradiance data. 4 ed. Geneva (Switzerland): International Electrotechnical Commission IEC, https://webstore.iec.ch/publication/61084; 2019.
19. Arora ND, Hauser JR. Temperature dependence of silicon solar cell characteristics. *Sol Energ Mater*. 1982;6(2):151-158. https://doi.org/10.1016/0165-1633(82)90016-8
20. Fan JCC. Theoretical temperature dependence of solar cell parameters. *Sol Cells*. 1986;17(2):309-315. https://doi.org/10.1016/0379-6787(86)90020-7
21. Emery KA, Osterwald CR. Solar cell efficiency measurements. *Sol Cells*. 1986;17(2):253-274. https://doi.org/10.1016/0379-6787(86)90016-5
22. Landis GA. Review of solar cell temperature coefficients for space. In: 13th Space Photovoltaic Research and Technology Conference SPRAT No. N95-20514; 1994:385-399. https://ntrs.nasa.gov/search.jsp?R=19950014125
23. Makrides G, Zinsser B, Georghiou GE, Schubert M, Werner JH. Temperature behaviour of different photovoltaic systems installed in Cyprus and Germany. *Sol Energ Mat Sol C*. 2009;93(6):1095-1099. https://doi.org/10.1016/j.solmat.2008.12.024
24. Smith RM, Jordan DC, Kurtz SR. Outdoor PV module degradation of current–voltage parameters. In: World Renewable Energy Forum No. NREL/CP-5200-53713; 2012; Denver (CO, USA). https://www.nrel.gov/docs/fy12osti/53713.pdf
25. Granata JE, Boyson WE, Kratochvil JA, Li B, Abbaraju V, Tamizh-Mani G, et al. Successful transfer of Sandia National Laboratories' outdoor test technology to TÜV Rheinland Photovoltaic Testing Laboratory. In: 37th IEEE Photovoltaic Specialists Conference PVSC; 2011:3132-3137. https://doi.org/10.1109/PVSC.2011.6186606
26. Cotfas DT, Cotfas PA, Machidon OM. Study of temperature coefficients for parameters of photovoltaic cells. Int J Photoenergy, https://doi.org/10.1155/2018/5945602; 2018.
27. Cotfas PA, Cotfas DT. Design and implementation of RELab system to study the solar and wind energy. *Measurement*. 2016;93:94-101. https://doi.org/10.1016/j.measurement.2016.06.060
28. Desharnais RA. Characterizing the impact of potential–induced degradation and recovery on the irradiance and temperature dependence of photovoltaic modules. In: 29th European Photovoltaic Solar Energy Conference and Exhibition EU PVSEC; 2014:2346-2350. https://doi.org/10.4229/EUPVSEC20142014-5CO.14.4
29. Spataru S, Hacke P, Sera D, Packard C, Kerekes T, Teodorescu R. Temperature–dependency analysis and correction methods of in situ power–loss estimation for crystalline silicon modules undergoing potential–induced degradation stress testing. *Prog Photovol Res Appl*. 2015;23(11):1536-1549. https://doi.org/10.1002/pip.2587
30. Islam MA, Hasanuzzaman M, Rahim NA. A comparative investigation on in–situ and laboratory standard test of the potential induced degradation of crystalline silicon photovoltaic modules. *Renew Energ*. 2018;127:102-113. https://doi.org/10.1016/j.renene.2018.04.051
31. Berthod C, Strandberg R, Odden JO, Sætre TO. Reduction of temperature coefficients in multicrystalline silicon solar cells after light–induced degradation. In: 42nd IEEE Photovoltaic Specialist Conference PVSC New Orleans. LA USA; 2015:1-5. https://doi.org/10.1109/PVSC.2015.7355753
32. Características Módulo Fotovoltaico I–53. 7 ed. Málaga (Spain): Isofotón S.A., https://www.dropbox.com/s/719xnjopgm46ujp/i53.pdf; 2003.
33. Piliougine M, Carretero J, Mora-López L, Sidrach-de-Cardona M. Experimental system for current–voltage curve measurement of photovoltaic modules under outdoor conditions. *Prog Photovol Res Appl*. 2011;19(5):591-602. https://doi.org/10.1002/pip.1073
34. Piliougine M, Carretero J, Mora-López L, Sidrach-de-Cardona M. New software tool to characterize photovoltaic modules from commercial equipment. WEENTECH Proceedings in Energy, 211–220, https://doi.org/10.32438/WPE.6218; 2018.
35. IEC 60904–1. Photovoltaic devices—Part 1: Measurement of photovoltaic current–voltage characteristics. 3 ed. Geneva (Switzerland): International Electrotechnical Commission IEC, https://webstore.iec.ch/publication/32004; 2020.
36. IEC 61853–1. Photovoltaic (PV) module performance testing and energy rating—Part 1: Irradiance and temperature performance measurements and power rating. 1 ed. Geneva (Switzerland): International Electrotechnical Commission IEC, https://webstore.iec.ch/publication/6035; 2011.
37. Dunn L, Gostein M, Emery K. Comparison of pyranometers vs. PV reference cells for evaluation of PV array performance. In: 38th IEEE Photovoltaic Specialists Conference PVSC; 2012:2899-2904.
38. Whitfield K, Osterwald CR. Procedure for determining the uncertainty of photovoltaic module outdoor electrical performance. *Prog Photovol Res Appl*. 2001;9(2):87-102. https://doi.org/10.1002/pip.356
39. Emery K. Photovoltaic calibrations at the National Renewable Energy Laboratory and uncertainty analysis following the ISO 17025 guidelines. No. NREL/TP-5J00-66873, Golden (CO, USA): National Renewable Energy Laboratory NREL, https://www.nrel.gov/docs/fy17osti/66873.pdf; 2016.
40. Piliougine M, Guejia-Burbano RA, Petrone G, Sánchez-Pacheco FJ, Mora-López L, de Cardona MS. Parameters extraction of single diode model for degraded photovoltaic modules. *Renew Energ*. 2021;164:674-686. https://doi.org/10.1016/j.renene.2020.09.035

41. Carlsson T, Åström K, Konttinen P, Lund P. Data filtering methods for determining performance parameters in photovoltaic module field tests. *Prog Photovol Res Appl*. 2006;14(4):329-340. https://doi.org/10.1002/pip.669
42. Agilent 34410A/11A Multimeter User's Guide. 5 ed. Santa Clara (CA, USA): Agilent Technologies. https://www.dropbox.com/s/wsvrsam9sd1av7r/Agilent34411A.pdf?dl=0; 2012.
43. ISO/IEC Guide 98-3. Uncertainty of measurement--Part 3: Guide to the expression of uncertainty in measurement (GUM:1995). 1 ed. Geneva (Switzerland): International Organization for Standardization ISO, https://www.iso.org/standard/50461.html; 2008.
44. York D, Evensen NM, Martınez ML, De Basabe Delgado J. Unified equations for the slope, intercept, and standard errors of the best straight line. *Am J Phys*. 2004;72(3):367-375. https://doi.org/10.1119/1.1632486
45. Wiens T. Linear regression with errors in X and Y. https://www.mathworks.com/matlabcentral/fileexchange/26586-linear-regression-with-errors-in-x-and-y, MATLAB Central File Exchange. Last visited: 14/10/2020; 2010.
46. Cox MG, Siebert BRL. The use of a Monte Carlo method for evaluating uncertainty and expanded uncertainty. *Metrologia*. 2006;43(4):S178-S188. https://doi.org/10.1088/0026-1394/43/4/s03
47. Robens C. Monte Carlo error propagation. https://www.mathworks.com/matlabcentral/fileexchange/57672-monte-carlo-error-propagation, MATLAB Central File Exchange. Last visited: 14/10/2020; 2016.
48. FieldPoint Operating Instructions FP-RTD-124 and cFP-RTD-124. Austin (TX, USA): National Instruments, https://www.dropbox.com/s/gtodukvcxh5rf9m/cFP_RTD_124.pdf; 2002.
49. Müllejans H, Zaaiman W, Galleano R. Analysis and mitigation of measurement uncertainties in the traceability chain for the calibration of photovoltaic devices. *Meas Sci Technol*. 2009;20(7):75101. https://doi.org/10.1088/0957-0233/20/7/075101
50. FieldPoint Operating Instructions FP-AI-112 and cFP-AI-112. Austin (TX, USA), National Instruments, https://www.dropbox.com/s/6ik30bq6ar7qs06/cFP_AI_112.pdf; 2004.
51. Singh P, Singh SN, Lal M, Husain M. Temperature dependence of I-V characteristics and performance parameters of silicon solar cell. *Sol Energ Mat Sol C*. 2008;92(12):1611-1616. https://doi.org/10.1016/j.solmat.2008.07.010
52. Dirnberger D., Bartke J., Steinhüser A., Kiefer K., Neuberger F. Uncertainty of field I-V curve measurements in large scale PV systems. In: 25th European Photovoltaic Solar Energy Conference and Exhibition EU PVSEC / 5th World Conference on Photovoltaic Energy Conversion WCPEC; 2010:4587-4594. https://doi.org/10.4229/25thEUPVSEC2010-4BV.1.62
53. Fanney AH, Dougherty BP, Davis MW. Short-term characterization of building integrated photovoltaic panels. *J Sol Energy Eng, 01*. 2003;125(1):13-20. https://doi.org/10.1115/1.1531642
54. Huang BJ, Yang PE, Lin YP, Lin BY, Chen HJ, Lai RC, et al. Solar cell junction temperature measurement of PV module. *Sol Energy*. 2011;85(2):388-392. https://doi.org/10.1016/j.solener.2010.11.006
55. Berthod C, Strandberg R, Yordanov GH, Beyer HG, Odden JO. On the variability of the temperature coefficients of mc–Si solar cells with irradiance. *Energy Procedia*. 2016;92:2-9. https://doi.org/10.1016/j.egypro.2016.07.002
56. Bensalem S, Chegaar M, Aillerie M. Solar cells electrical behavior under thermal gradient. *Energy Procedia*. 2013;36:1249-1254. https://doi.org/10.1016/j.egypro.2013.07.141
57. Mihaylov B, Betts TR, Pozza A, Müllejans H, Gottschalg R. Uncertainty estimation of temperature coefficient measurements of PV modules. *IEEE J Photovolt*. 2016;6(6):1554-1563. https://doi.org/10.1109/JPHOTOV.2016.2598259

How to cite this article: Piliougine M, Oukaja A, Sidrach-de-Cardona M, Spagnuolo G. Temperature coefficients of degraded crystalline silicon photovoltaic modules at outdoor conditions. *Prog Photovolt Res Appl*. 2021;29:558-570. https://doi.org/10.1002/pip.3396